

# Distribution of Myocilin and Extracellular Matrix Components in the Corneoscleral Meshwork of Human Eyes

Jun Ueda and Beatrice Y. J. T. Yue

**PURPOSE.** To examine ultrastructurally the composition of major extracellular matrix (ECM) components and the distribution of myocilin in the trabecular lamellae of corneoscleral (CS) meshwork in normal human eyes. The codistribution of myocilin with ECM components was also investigated.

**METHODS.** Postembedding immunoelectron microscopic studies were performed with antibodies against myocilin and other ECM components, including fibronectin, laminin, vitronectin, tenascin, elastin, fibrillin-1, microfibril-associated glycoprotein (MAGP)-1, decorin, versican, hyaluronic acid, and five types of collagen (I, III, IV, V, and VI). Double labeling of myocilin with other ECM components was performed with different sized gold particles.

**RESULTS.** In the trabecular beams of CS meshwork, fibronectin, laminin, and collagen type IV were associated with basement membranes, whereas elastin was specifically localized to the core of elastic-like fibers. Several types of collagens, glycoproteins, proteoglycans, and hyaluronic acid were detected both in the collagen fibers and ground substances. Myocilin predominantly localized in the long-spacing collagens and sheath materials surrounding elastic-like fibers, codistributed with fibronectin, fibrillin-1, MAGP-1, decorin, and type VI collagen.

**CONCLUSIONS.** This study illustrated the composition of ECM materials in the trabecular lamellae of CS meshwork. Myocilin was specifically localized to long-spacing collagens and the surrounding sheath of elastic-like fibers interacting with microfibril-associated elements where changes have been documented to occur in glaucomatous and aging eyes. (*Invest Ophthalmol Vis Sci.* 2003;44:4772-4779) DOI:10.1167/iov.02-1002

Myocilin,<sup>1</sup> also known as trabecular meshwork-inducible glucocorticoid response (TIGR), was originally cloned from cultured human trabecular meshwork (TM) cells as a protein upregulated by dexamethasone treatment.<sup>2,3</sup> This gene has been directly linked<sup>4</sup> to both juvenile- and adult-onset primary open-angle glaucoma (POAG). Approximately 3% to 4% of patients with POAG have been found to have mutations in this gene, irrespective of region or race.<sup>5-7</sup>

In humans, myocilin is expressed in several ocular and nonocular tissues.<sup>8</sup> The expression level of myocilin in the TM appears to be considerably higher than in other ocular tissues.

In situ hybridization experiments also indicate that the mRNA levels are similar in the uveal, corneoscleral (CS), and juxtacanalicular (JCT) regions of TM tissues.<sup>9-13</sup> The physiologic functions of myocilin and its precise roles in the pathogenesis of glaucoma nevertheless remain largely a mystery.<sup>8</sup> We have demonstrated by immunoelectron microscopy that myocilin is localized both intracellularly and extracellularly to multiple sites in normal human TM tissues and in cultured cells.<sup>14</sup> Intracellularly, myocilin is associated with mitochondria, vesicles, centrosomes, and cytoplasmic filaments, including actin stress fibers and intermediate filaments. Extracellularly, it is localized in TM tissues in association with the extracellular matrix (ECM).

In a subsequent investigation,<sup>15</sup> we examined the extracellular localization of myocilin in the JCT connective tissue of TM. Myocilin was demonstrated to localize predominantly to the microfibrillar architectures of sheath-derived (SD) plaque materials, within the clusters of the banded material surrounding the plaques. This distribution pattern is intriguing, because the microfibrillar structure is the most prominent ECM component in the region and abnormal accumulation of SD plaques has been established as a characteristic pathologic change observed in the JCT of patients with POAG.<sup>16-22</sup>

The CS meshwork portion of TM tissues extends approximately 100  $\mu\text{m}$  in the direction of the aqueous flow and consists of interconnecting sheets of trabecular beams that contain lamellae of connective tissue elements.<sup>22,23</sup> Cells in the CS meshwork line the trabecular beams. This contrasts with that in the JCT region, where cells reside relatively freely and are embedded in connective tissues. The JCT/Schlemm's canal area is believed to be the main site of resistance of the aqueous outflow. The TM cells covering the corneoscleral beams nevertheless are also likely to have their roles in maintenance of the normal outflow. For instance, TM cells are known to engulf debris in a self-cleaning manner,<sup>24</sup> so that the pathways remain free for the fluid to flow through the meshwork.

Underneath the TM cells in the CS meshwork, there are basement membranes. The beams or trabecular cores are made up essentially of collagen fibers embedded in ground substances as a matrix, and elastic-like fibers as a plexiform framework. In trabecular lamellae, the accumulation of "long-spacing collagens" and thickening of basement membranes are well-documented changes in aged eyes.<sup>25</sup> Long-spacing collagen is also observed in the eyes of patients with POAG.<sup>16</sup> It is characterized as a cross-banded structure with approximately 100 to 120 nm periodicity,<sup>26</sup> which is longer than that (52-62 nm) of collagen types I and III. The exact nature of this structure has yet to be clearly defined.

In this study, we continued our efforts, analyzing systematically the ECM composition of the basement membrane, the trabecular core and the long-spacing collagens in the CS meshwork of normal human eyes. A postembedding colloidal gold immunoelectron microscopy (immuno-EM) method was used. The TM sections were immunostained with antibodies specific for major ECM components of TM including fibronectin, laminin, vitronectin, tenascin, elastin, fibrillin-1, microfibril-associated

---

From the Department of Ophthalmology and Visual Sciences, University of Illinois at Chicago College of Medicine, Chicago, Illinois. Supported by Grants EY05628 and EY03890 and Core Grant EY01792 from the National Eye Institute and the Japan Foundation for Aging and Health, Aichi, Japan.

Submitted for publication September 30, 2002; revised March 12 and April 8, 2003; accepted April 21, 2003.

Disclosure: **J. Ueda**, None; **B.Y.J.T. Yue**, None

The publication costs of this article were defrayed in part by page charge payment. This article must therefore be marked "advertisement" in accordance with 18 U.S.C. §1734 solely to indicate this fact.

Corresponding author: Beatrice Yue, University of Illinois at Chicago, Department of Ophthalmology and Visual Sciences, 1855 W. Taylor Street, Chicago, IL 60612; u24184@uic.edu.

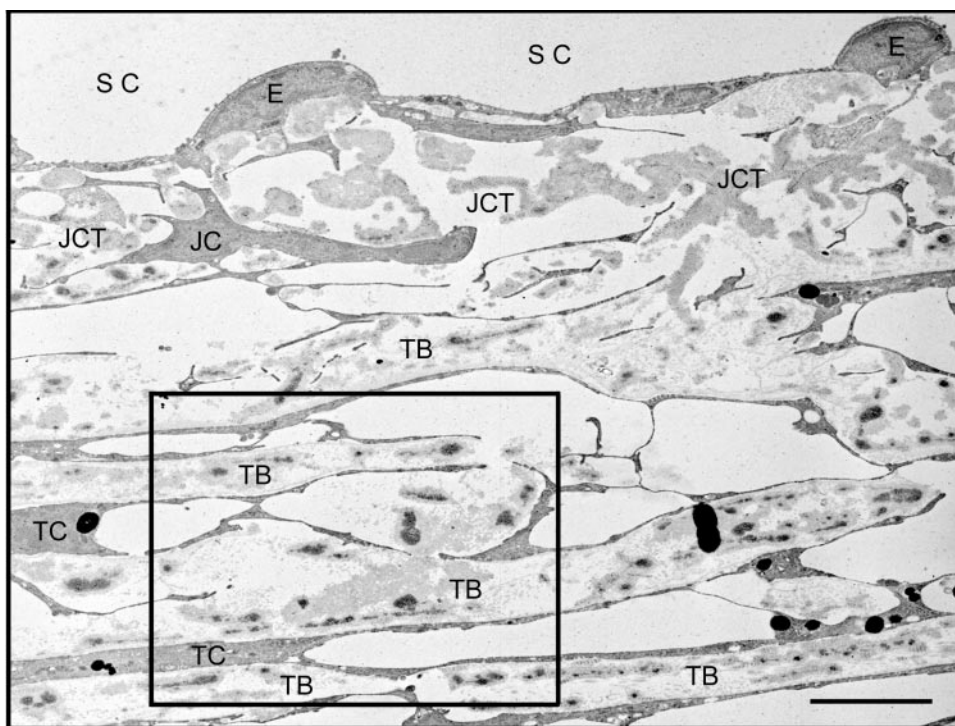


**FIGURE 1.** A low-magnification micrograph demonstrating the CS meshwork structure. The CS meshwork, underneath Schlemm's canal (SC) and the JCT area, is composed of interconnecting sheets of trabecular beams (TB). Trabecular cells (TC) line the beams. Cells (JC) in the JCT area are, by contrast, embedded in connective tissues. The boxed area in the CS meshwork was examined by immunogold electron microscopy. E, SC cells. Bar, 5  $\mu$ m.

ated glycoprotein (MAGP)-1, decorin, versican, hyaluronic acid, and five types of collagen (I, III, IV, V, and VI).

The extracellular localization of myocilin in this region was also investigated. In addition, double labeling was performed to determine whether, and which, ECM components colocalize with myocilin in the trabecular lamellae of CS meshwork.

## MATERIALS AND METHODS

Six normal human donor eyes (donor ages, 39, 47, 48, 58, 72, and 74 years) with no history of glaucoma or other eye diseases were obtained from the Illinois Eye Bank at Chicago within 24 hours of death. The procurement of tissues was approved by the Institutional Review Board at the University of Illinois at Chicago and complied with the Declaration of Helsinki. TM tissues isolated were fixed for 3 hours in 4% paraformaldehyde and 0.1% glutaraldehyde in 0.1 M phosphate buffer (pH 7.4). The specimens were dehydrated at  $-20^{\circ}\text{C}$  through a graded series of *N,N*-dimethylformamide and were finally immersed in a glycol methacrylate embedding medium. They were subsequently polymerized by ultraviolet irradiation at  $-20^{\circ}\text{C}$  for 48 hours. Ultrathin 80-nm serial sections were obtained through the entire layers of TM, and were mounted on 150-mesh nickel grids.

To minimize nonspecific binding, sections were blocked at room temperature (RT) in 1% bovine serum albumin in phosphate-buffered saline (PBS) for 15 minutes. The grids were then incubated at RT with a specific primary antibody for 3 hours. The primary antibodies were rabbit anti-human fibronectin (1:20 in the blocking buffer; ICN Biochemicals, Irvine, CA), laminin (1:15; Sigma-Aldrich, St. Louis, MO), tenascin (1:20; Invitrogen-Life Technologies, Gaithersburg, MD), elastin (1:150; Elastin Products Co., Owensville, MO), fibrillin-1 (1:150; Elastin Products Co.), MAGP-1 (1:200; Elastin Products Co.), and collagen types I (1:20; Chemicon, Temecula, CA), III (1:40; Chemicon), and IV (1:20; Collaborative Research, Bedford, MA); mouse anti-human vitronectin (1:20; Invitrogen-Life Technologies), versican (1:15; Seikagaku Corp., Falmouth, MA), and collagen types V and VI (1:15; Chemicon); and sheep anti-human decorin (1:500; United States Biological, Swampscott, MA). Several dilutions of the antibodies were tested, and the optimal one was chosen for the study. An affinity-purified polyclonal antibody anti-myocilin-33 was also used as a primary antibody at

a dilution of 1:200. The development and specificity of this antibody were as previously described.<sup>14,15</sup>

After the primary antibody incubation, the grids were rinsed thoroughly in a mixture of 0.05% Tween-20 in PBS. The sections were further incubated with 12-nm colloidal gold-conjugated goat anti-rabbit (1:50; Jackson ImmunoResearch, West Grove, PA) goat anti-mouse IgG (1:30; Jackson ImmunoResearch), or 6-nm colloidal gold-conjugated donkey anti-sheep IgG (1:100; Jackson ImmunoResearch) at RT for 1 hour. The sections were then rinsed, stained with uranyl acetate, and examined under a transmission electron microscope (model JEM-1220; JEOL, Peabody, MA) at 80 kV accelerating voltage. As a negative control, normal rabbit, mouse, or sheep IgG or anti-myocilin preadsorbed with the immunogenic peptide was used instead of the primary antibody at the equivalent concentration of IgG fraction.

To localize hyaluronic acid, the sections were incubated with biotinylated hyaluronic acid binding protein (HABP; 1:10; United States Biological) after blocking. The sections were next incubated for 1 hour in horseradish peroxidase (HRP)-conjugated streptavidin (1:50; Jackson ImmunoResearch) and for another hour in 6-nm colloidal gold-conjugated goat anti-HRP (1:20; Jackson ImmunoResearch).

To determine the relative distribution of each of the 16 molecules, the intensity of immunogold labeling or the amount of gold particles in each ECM structure was graded. More than 10 micrographs from each eye were examined by two masked observers. The intensity was scored from  $\pm$  to  $+++$ , with  $\pm$  representing minimal staining and  $+++$ , intense staining.

To examine the interaction between myocilin and other ECM components, double labeling was performed. One side of the section was immunostained for myocilin and labeled with 12-nm gold particles, and the other side was stained for ECM elements with 6-nm gold particles. Single-side incubation was achieved by floating the grids on a drop of each solution.

## RESULTS

### Immunogold Labeling of Major ECM Components in the CS Meshwork

The CS meshwork is composed of interconnecting sheets of trabecular beams with TM cells lining the beams. Figure 1

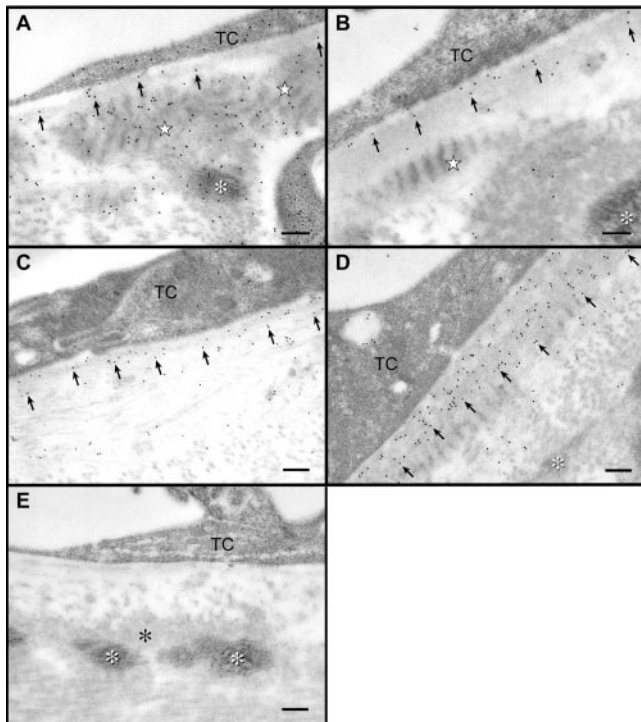


**FIGURE 2.** Immunogold localization of ECM elements in basement membranes of the CS meshwork. (A) Moderate labeling for fibronectin was observed in basement membranes (arrows) underneath trabecular cells (TC), the long-spacing collagens (stars), and the sheath materials surrounding the elastic core (white asterisk). Intracellular labeling, as was reported in the literature,<sup>15,27,28</sup> was also observed. (B) Labeling for laminin was noted in the basement membranes (arrows) and the sheath materials, but not in the long-spacing collagens (star). (C) Strong labeling for collagen type IV was found in basement membranes (arrows). (D) Labeling for collagen type IV was demonstrated in thickened basement membranes (arrows) underneath the lining of TM cells, but not in elastic-like fibers (white asterisk). (E) When the primary antibody was replaced with rabbit IgG, the gold labeling was negligible. TC, trabecular cells; white asterisk: core of elastic-like fibers; black asterisk, sheath of elastic fibers. Bar, 200 nm.

shows a low-magnification micrograph demonstrating structure of the CS meshwork underneath Schlemm's canal and the JCT region. The boxed area in the CS meshwork was examined by immunogold EM in the present study.

### Basement Membranes

In the trabecular lamellae of normal human eyes, moderate immunogold labeling for fibronectin (Fig. 2A) was noted in the basement membranes. Abundant labeling for laminin (Fig. 2B) and collagen type IV (Fig. 2C) was also observed. Occasionally, thickened basement membranes were observed underneath the lining of TM cells, and collagen type IV (Fig. 2D), laminin and fibronectin (data not shown) were seen decorating the entire layer of this structure. Other ECM proteins were minimally detected (Figs. 3, 4, 5) in the basement membranes. The gold labeling was negligible when normal rabbit IgG was used instead of the primary antibody (Fig. 2E). In addition, it is addition of note that fibronectin was found not only underneath the TM cell lining, but also within the sheath materials of elastic-like fibers (Figs. 2A, 4A) and the long-spacing collagens (Fig. 6A). Laminin was in the sheath materials, but not in the long-spacing collagens (Fig. 2B). Intracellular labeling was observed, as also has been reported in the literature.<sup>15,27,28</sup>

### Trabecular Cores

The collagen fibers embedded in the ground substance were immunolabeled for collagen types I (Fig. 3A) and V (Fig. 3B). Core elastic-like fibers were composed of electron-dense and electron-lucent areas, and were surrounded by microfibrillar sheath materials. Elastin, as has been shown,<sup>15,29</sup> was immunolocalized almost exclusively to the region within or adjacent to the electron-lucent area of the core (Figs. 3C). Other ECM substances (Figs. 4, 5) including fibrillin-1,<sup>30</sup> MAGP-1<sup>31</sup> (data not shown), fibronectin,<sup>32</sup> decorin,<sup>33,34</sup> collagen types III (data not shown) and VI, vitronectin, tenascin, versican, and hyaluronic acid were observed both in the core and the surrounding sheath. Fibronectin (Fig. 4A) and collagen type III (data not shown) were more densely distributed in the sheath area. Fibrillin-1 (Fig. 4B), decorin (Fig. 4C), collagen type VI (Fig. 4D), vitronectin (Fig. 5A), tenascin (Fig. 5B), versican (Fig. 5C), and hyaluronic acid (Fig. 5D) were by contrast, more abundantly distributed in the core of elastic-like fibers. Negative controls using normal mouse IgG (Fig. 3D) and sheep IgG (data not shown) showed minimal staining.

### Long-Spacing Collagens

In the donor eyes examined, long-spacing collagens, the electron-dense bands with a periodicity of 100 to 120 nm, were observed both adjacent to the sheath of elastic-like fibers and/or embedded in the ground substances. This structure was specifically immunolabeled by fibronectin (Fig. 6A), fibrillin-1 (Fig. 6B), decorin (Fig. 6C), and collagen type VI (Fig. 6D). Vitronectin, versican, and tenascin (data not shown) were also detected within the deposits, although they were not specifically localized to the electron-dense bands.

The intensity of immunogold labeling in each ECM structure was graded from  $\pm$  to  $+++$ , with  $\pm$  representing minimal, and  $+++$ , intense staining. The labeling intensity and the labeling pattern for all the ECM components examined are summarized in Table 1. Results from TM tissues of six donors were essentially identical.

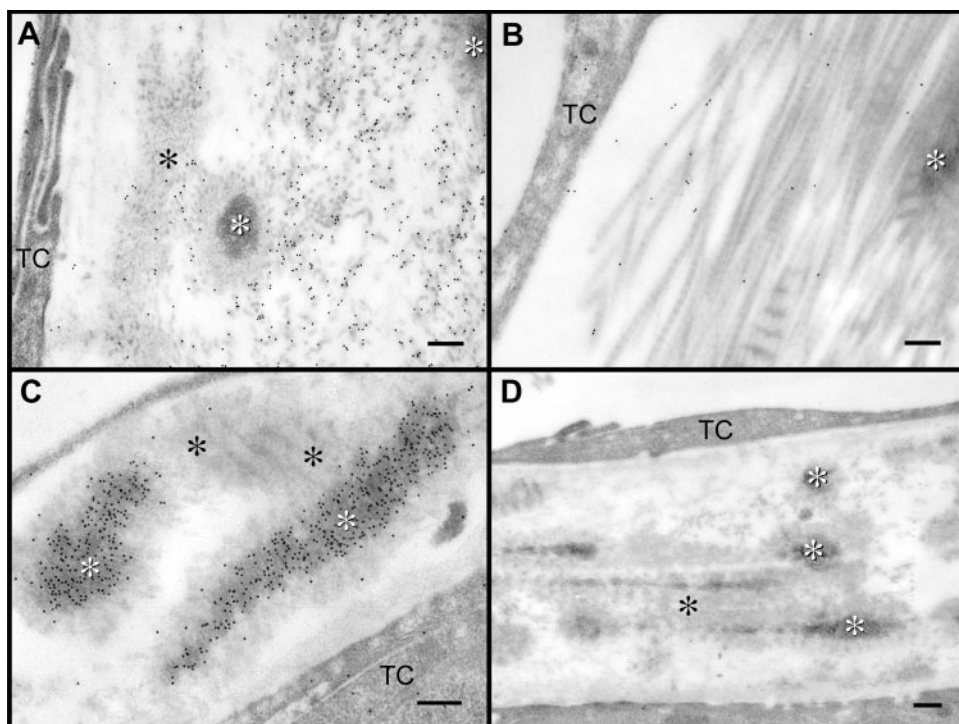
### Immunogold Labeling of Myocilin in the CS Meshwork

Immunogold labeling using an affinity-purified anti-myocilin antibody showed that the gold particles were heavily localized to the sheath materials surrounding elastic-like fibers (Figs. 7A, 7B) and the long-spacing collagens (Figs. 7A, 7C). Myocilin was also found, as expected, in the cells, and sparsely associated with collagen fibers embedded in ground substances. In the basement membrane, gold particles representing myocilin were barely detectable. When the peptide-adsorbed anti-myocilin (Fig. 7D) was used in negative control experiments, the gold labeling was at a minimum. A summary of the myocilin distribution in each ECM structure is presented in Table 1.

### Double Labeling of Myocilin and Other ECM Proteins

Immunogold double labeling with myocilin was performed, using different sized gold particles. Codistribution of myocilin (12 nm-gold particles) with fibronectin (6 nm, Fig. 8A), fibrillin-1 (6 nm, Fig. 8B), MAGP-1 (6 nm, Fig. 8C), and decorin (6 nm, Fig. 8D), was demonstrated. The distribution of myocilin and collagen type VI also overlapped (compare Figs. 7B and 7C with Figs. 4D and 6D). All these molecules were heavily associated with long-spacing collagens and microfibrillar architecture of sheath materials. In addition, minor codistribution of myocilin was noted with other components in the sheath such as vitronectin, tenascin, laminin, and hyaluronic acid (data not shown).

**FIGURE 3.** Immunogold labeling of ECM components in trabecular cores. Trabecular cores were made up of ground substances with collagen fibers as a matrix and elastic-like fibers as a plexiform framework. Collagen fibers were strongly immunolabeled for collagen type I (A) and moderately for collagen type V (B). Core elastic-like fibers (*white asterisks*) were composed of electron-dense and electron-lucent areas and were surrounded by microfibrillar sheath materials (*black asterisks*). Elastin was immunolocalized almost exclusively to the region within or adjacent to the electron-lucent area of the core (C). Minimal staining was observed in mouse IgG negative control (D). TC, trabecular cell. Bar, 200 nm.



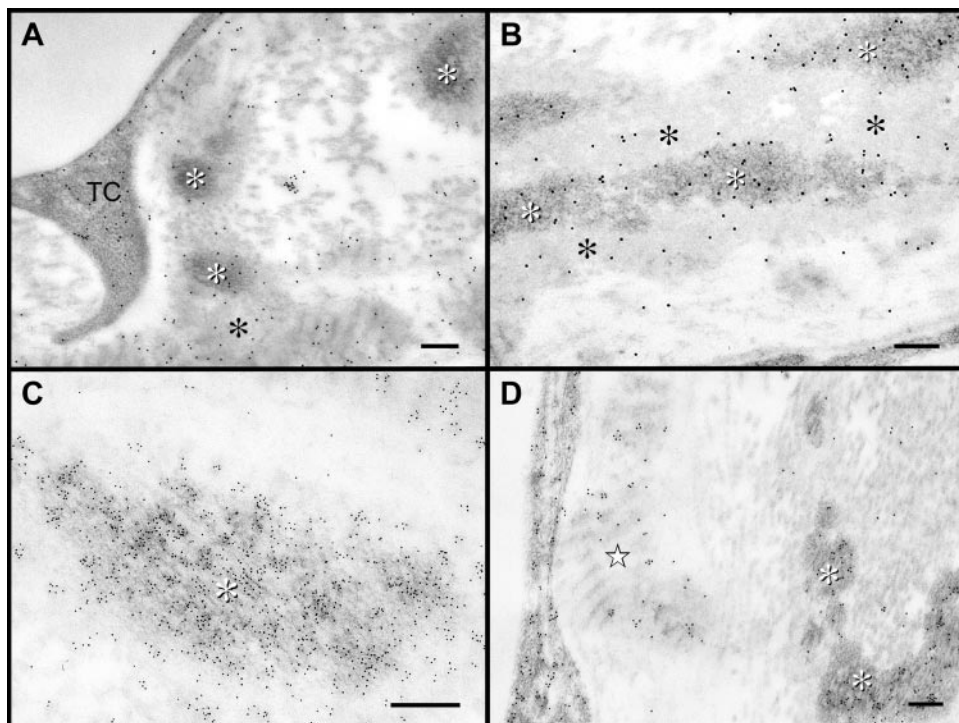
## DISCUSSION

In the present study, we comprehensively analyzed the ECM composition of the structures within trabecular lamellae in the CS meshwork of normal human TM tissues. The ultrastructural distribution of three elastic fiber-associated molecules (elastin, fibrillin-1 and MAGP-1), four glycoproteins (fibronectin, laminin, vitronectin and tenascin), two proteoglycans (decorin and versican), five types of collagen (I, III, IV, V, and VI), and hyaluronic acid was examined. Studies of proteins such as fibronectin, elastin, and collagen types I and III (data not

shown) confirmed previous results.<sup>28,29,35-38</sup> Moreover, novel information regarding distribution of several molecules including vitronectin, tenascin, and versican was obtained. The precise extracellular localization of myocilin in the CS meshwork was also determined.

In the CS meshwork, the basement membrane of the trabecular lamellae was found to immunolabel abundantly for collagen type IV and laminin and moderately for fibronectin. The label was observed over the full thickness of the basement membranes. Fibronectin was noted in addition within the sheath material of elastic-like fibers. To a lesser degree, the

**FIGURE 4.** In the elastic-like fibers of trabecular lamellae, staining for ECM components including fibronectin (A), fibrillin-1 (B), decorin (C), and collagen type VI (D) was observed, both in the core (*white asterisks*) and the surrounding sheath (*black asterisks*). Fibronectin (A) was more densely distributed in the sheath area. Fibrillin-1 (B), decorin (C), and collagen type VI (D) were, by contrast, more abundantly distributed in the core of elastic-like fibers. Mild labeling for collagen type VI (D) was seen in long-spacing collagens (*star*). Intracellular grains were also observed. TC, trabecular cell. Bar, 200 nm.



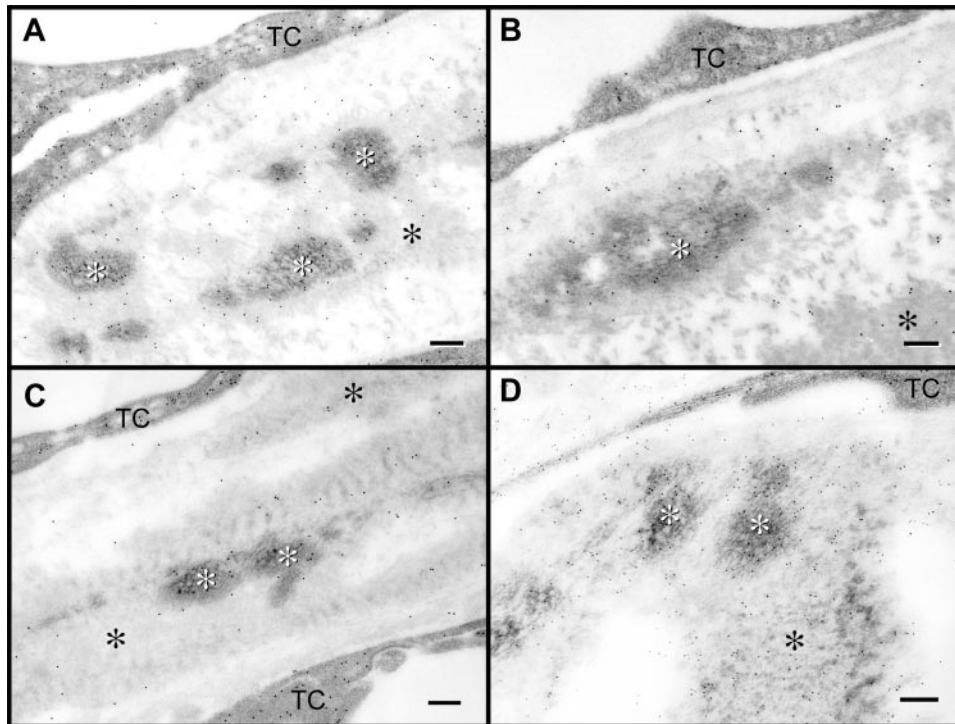


**FIGURE 5.** In the elastic-like fibers of trabecular lamellae, vitronectin (A), tenascin (B), versican (C), and hyaluronic acid (D) were localized both in the core (*white asterisks*) and the surrounding sheath (*black asterisks*). These molecules were in general more abundantly distributed in the core of elastic-like fibers. TC, trabecular cells. Bar, 200 nm.

sheath material was also labeled by anti-laminin but immunoreactivity toward anti-collagen type IV was virtually absent. These findings are in accordance with the ultrastructural distribution of fibronectin, laminin, and collagen type IV reported previously in immuno-EM investigations of normal and glaucomatous eyes.<sup>36,37</sup>

In the present EM study, collagen type I was mostly associated with collagen fibers in the ground substance, rather than with the basement membranes or the elastin-like fibers. This result agrees with and verifies the previously published EM<sup>37</sup> and light microscopic<sup>38</sup> data. Also in consistence with previous

results,<sup>37,38</sup> labeling for type III collagen was observed in the fibrillar-like material in the trabecular core. It should be noted that the antibody for collagen type III had minor cross-reactivity (<10%) toward type I collagen and vice versa. However, the differential distribution patterns of these collagen types and the reaffirmation of previous findings argue for the compelling representation of each collagen type by the gold labeling in the current investigation.

The so-called long-spacing collagens<sup>25,26</sup> are cross-striated fiber bundles, both in the ground substances and the sheath materials surrounding elastic-like fibers. Collagen type VI has

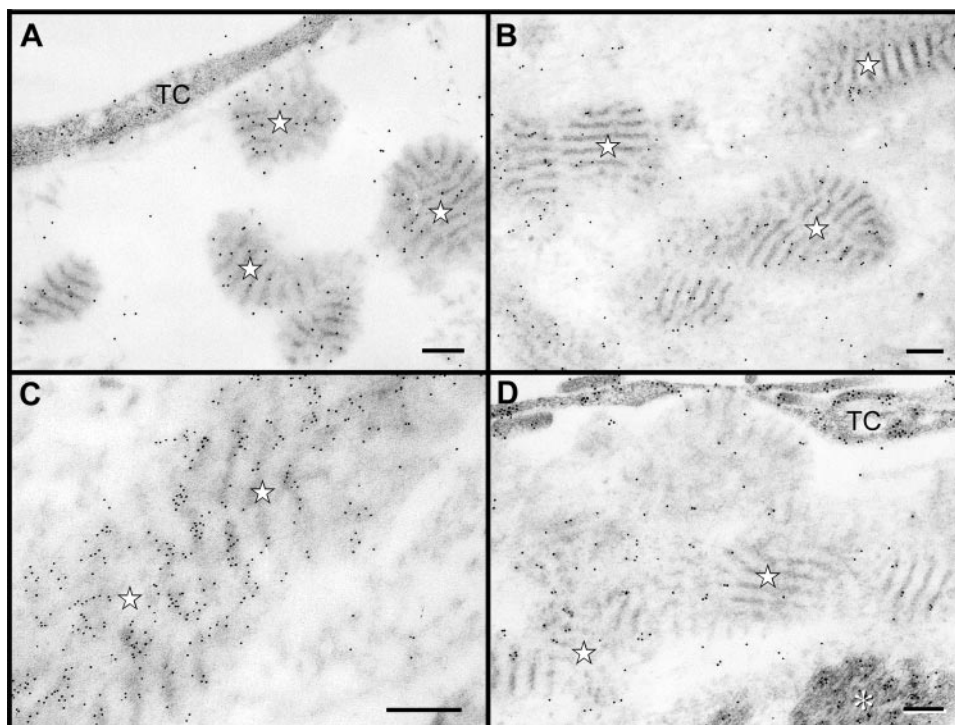


**FIGURE 6.** In the eyes of 58- and 72-year-old donors, long-spacing collagens (*stars*) were observed both adjacent to the sheath (*asterisk*) of elastic-like fibers and/or embedded in the ground substances. This structure was specifically immunolabeled by fibronectin (A), fibrillin-1 (B), decorin (C), and collagen type VI (D). TC, trabecular cells. Bar, 200 nm.

TABLE 1. Immunogold Labeling of ECM Components and Myocilin in the Trabecular Lamellae of the Corneoscleral Meshwork

	Basement Membrane	Collagen Fibers and Ground Substances	Core of Elastic-like Fibers	Sheath Material of Elastic-like Fibers	Long-Spacing Collagens
Fibronectin	++	+	+	++	+++
Vitronectin	±	+	++	+	+
Laminin	+++	±	±	+	±
Tenascin	±	+	++	+	+
Elastin	±	±	+++	+	±
Fibrillin-1	±	+	+++	++	++
MAGP-1	±	+	++	+	++
Versican	±	±	++	+	+
Decorin	±	+	+++	++	+++
Hyaluronic Acid	±	+	++	+	±
Collagen type I	±	+++	±	±	±
Collagen type III	±	+	+	++	+
Collagen type IV	+++	±	±	±	±
Collagen type V	±	++	±	±	±
Collagen type VI	±	±	+++	+	++
Myocilin	±	+	+	+++	+++

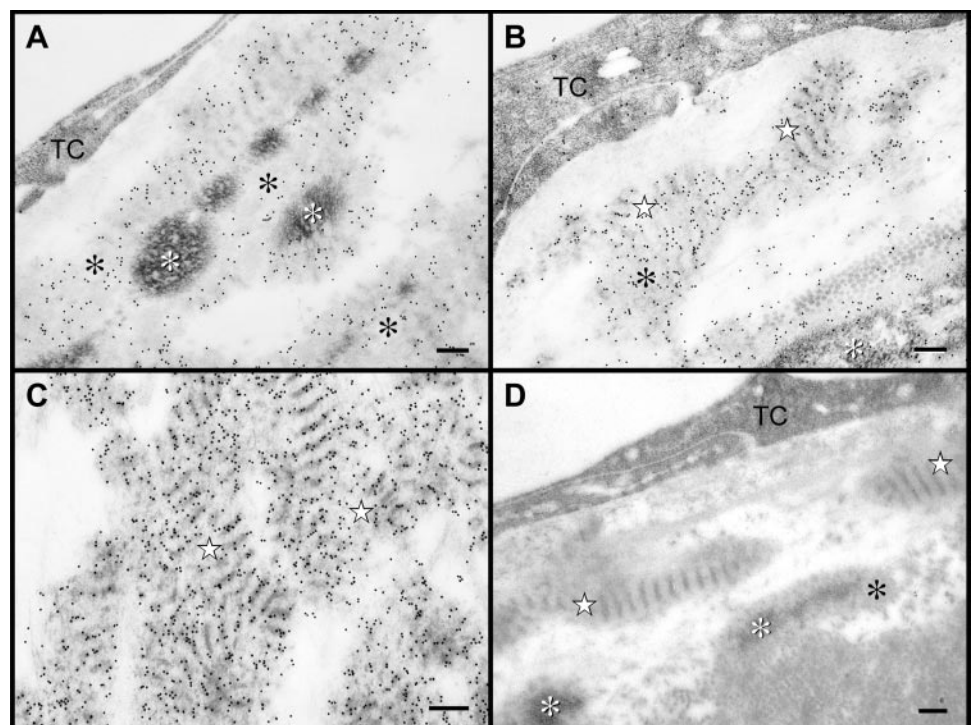
The intensity of immunogold labeling was graded in each ECM structure or plaques from ± to +++, with ± representing minimal, and +++, intense staining.

been shown to be one of the components of this structure in an earlier study by immunohistochemical and pre-embedding immuno-EM methods.<sup>26</sup> This observation however was disputed, as type VI collagen was not detected by cryoultramicrotomy in a subsequent investigation.<sup>37</sup> We confirmed the presence of collagen type VI (Fig. 6D) in the long-spacing collagens and further provided evidence that elements including fibronectin (Fig. 6A), fibrillin-1 (Fig. 6B), MAGP-1 (Fig. 8C), and decorin (Fig. 6C) are also constituents in these deposits. In particular, myocilin was found to be a major component distributed within the electron-dense cross bands (Fig. 7C). By immunoprecipitation, decorin has been shown to interact with fibrillin-1 and MAGP-1, forming a ternary complex.<sup>33,34</sup> Myocilin, in addition to being prone to form dimers and/or multimers,<sup>3,39,40</sup> is also capable of interacting with fibrillin-1, fibronectin, collagen type VI, and decorin.<sup>15</sup> The high molecular weight

myocilin may conceivably, through interactions with microfibrillar molecules, participate in the assembly of the fibers in long-spacing collagens. The myocilin localization on long-spacing collagens is in agreement with results of another pre-embedding immuno-EM study by Tawara et al.<sup>41</sup>

Besides long-spacing collagens, myocilin was also found localized in the CS meshwork to the sheath materials surrounding elastic-like fibers, codistributing with fibrillin-1, MAGP-1, and other sheath components such as decorin, vitronectin, tenascin, and versican. The myocilin distribution is distinct from that of elastin, which is localized predominantly in the elastic fiber core.<sup>15,31</sup> Myocilin labeling is also minimal in the basement membranes and hardly any codistribution is seen with collagen types I, IV, and V. The localization pattern for myocilin is very similar to that demonstrated in the JCT region.<sup>15</sup>

FIGURE 7. Immunogold labeling of myocilin in the CS meshwork. (A–C) Gold particles were heavily localized to the sheath materials (black asterisks) surrounding elastic-like fibers (white asterisks), and the long-spacing collagens (stars). Myocilin was also found, as expected in trabecular cells (TC), and sparsely in association with collagen fibers embedded in ground substances. In the thickened basement membrane, gold particles representing myocilin were barely detectable. (D) When the peptide-preabsorbed anti-myocilin was used to replace the primary antibody, almost no gold labeling was seen. Bar, 200 nm.



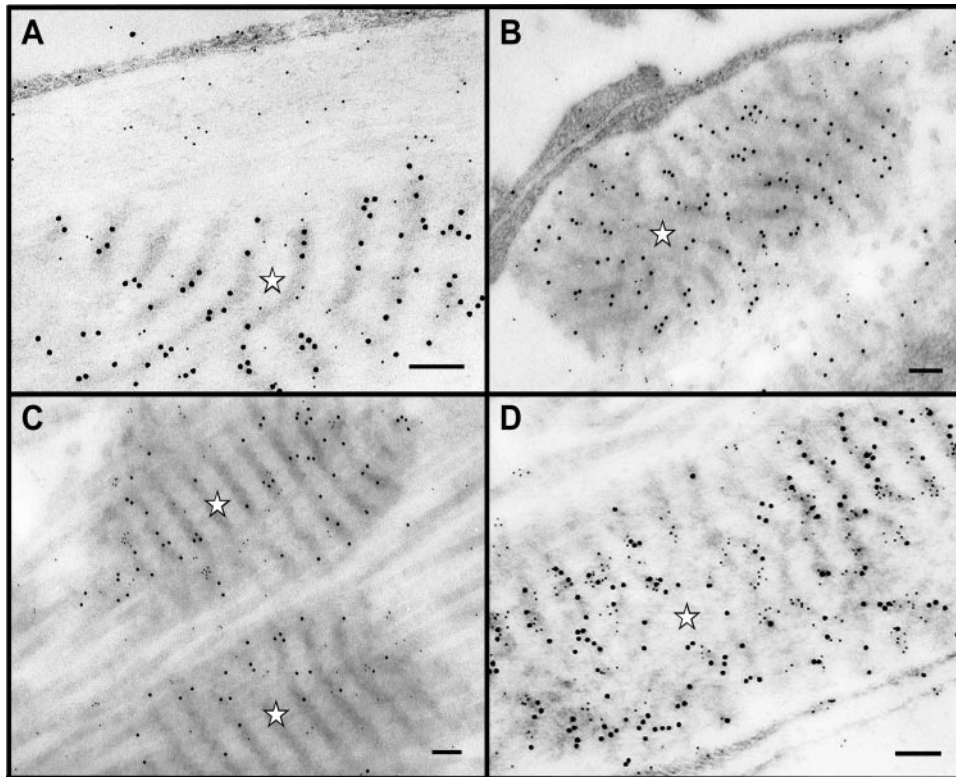


**FIGURE 8.** Double labeling of myocilin and ECM proteins in the CS meshwork. Major codistribution of myocilin (12-nm gold particles) with fibronectin (6 nm, **A**), fibrillin-1 (6 nm, **B**), MAGP-1 (6 nm, **C**), and decorin (6 nm, **D**) were demonstrated. These molecules and collagen type VI (Figs. 4D, 6D) were heavily associated with long-spacing collagens (*stars*) and the microfibrillar architecture of sheath materials. Bar, 100 nm.

Codistribution observed ultrastructurally does not necessarily indicate that interactions exist. Nevertheless, the current immuno-EM data concurs with our dot blot assay results,<sup>15</sup> showing myocilin codistribution and possible interactions with fibronectin and collagen type VI, but not with elastin or collagen type IV. In agreement with our data, interaction of myocilin with fibronectin was also noted by solid-phase binding assays by Filla et al.<sup>42</sup> Using recombinant fibronectin fragments, the heparin II domain of fibronectin was subsequently pinpointed as specific binding site for myocilin. This site is well known to have a role in cell adhesion, cytoskeleton structure, and signal transduction.<sup>43</sup> It was thus suggested that perhaps through the interaction with ECM molecules such as fibronectin, myocilin would have extracellular functions in the TM. Our localization findings further implicate that myocilin may have a role modulating the formation and/or assembly of ECM structures in the TM and may thereby regulate the aqueous outflow system. It is well documented<sup>16,25</sup> that changes in the myocilin-associated structures including an increase in the sheath materials surrounding elastic-like fiber network and accumulation of long-spacing collagens occur in trabecular beams of glaucomatous and aging eyes.

Little codistribution of myocilin with collagen types I and V was observed by immuno-EM, although our previous experiments disclosed their interactions with myocilin in dot blot assays *in vitro*.<sup>15</sup> These molecules may either be present in compartments different from myocilin or may be masked from myocilin binding *in situ*. Alternatively, findings of dot blot assays may be an artifact resulting from tests of denatured proteins. Our immunogold results also contrasted with that of immunofluorescence staining by Filla et al.,<sup>42</sup> who noted colocalization of myocilin with collagen type IV in cultured human TM cells. Because of the limited resolution, colocalization identified by light microscopy often must be substantiated by ultrastructural and biochemical studies. Because both our *in vitro* binding assay and the solid phase binding assays by Filla et al. showed no interaction between myocilin and collagen type IV,

the codistribution of immunofluorescence observed in their study may reflect mostly indirect associations.

Taken together, all evidence demonstrates the presence of type VI collagen in long-spacing collagens in the CS meshwork. Fibronectin, fibrillin-1, MAGP-1, decorin, and myocilin are also shown to be constituents of long-spacing collagens. Myocilin in addition is localized to the sheath materials surrounding elastic-like fibers in the CS meshwork, very similar to that observed in JCT regions. The myocilin localization is of significance because increased sheath materials and long-spacing collagens are frequently observed in the trabecular lamellae and JCT areas of POAG and aging eyes.<sup>16,25</sup> Myocilin may be one of the factors involved in the formation of glaucomatous deposits and age-related changes observed in both the trabecular beams and JCT. In this vein, it would be particularly interesting to analyze the distribution of upregulated myocilin in the TM of patients with steroid-induced glaucoma.<sup>44,45</sup> The ultrastructural localization of overexpressed myocilin in the various ECM structures or lack thereof may provide great insights into the role of myocilin in the development of glaucoma.

### Acknowledgments

The authors thank Kelly Wentz-Hunter for developing the primary antibody used in this study and Kira Lathrop for expert imaging advice.

### References

1. Kubota R, Noda S, Wang Y, et al. A novel myosin-like protein (myocilin) expressed in the connecting cilium of the photoreceptor: molecular cloning, tissue expression, and chromosomal mapping. *Genomics*. 1997;41:360-369.
2. Polansky JR, Fauss DJ, Chen P, et al. Cellular pharmacology and molecular biology of the trabecular meshwork inducible glucocorticoid response gene product. *Ophthalmologica*. 1997;211:126-139.
3. Nguyen TD, Chen P, Huang WD, Chen H, Johnson D, Polansky JR. Gene structure and properties of TIGR, an olfactomedin-related

- glycoprotein cloned from glucocorticoid-induced trabecular meshwork cells. *J Biol Chem*. 1998;273:6341-6350.
4. Stone EM, Fingert JH, Alward WLM, et al. Identification of a gene that causes primary open angle glaucoma. *Science*. 1997;275:668-670.
  5. Alward WL, Fingert JH, Coote MA, et al. Clinical features associated with mutations in the chromosome 1 open-angle glaucoma gene. *N Engl J Med*. 1998;338:1022-1027.
  6. Wiggs JL, Allingham RR, Vollrath D, et al. Prevalence of mutations in TIGR/Myocilin in patients with adult and juvenile primary open-angle glaucoma. *Am J Hum Genet*. 1998;63:1549-1552.
  7. Fingert JH, H'eon E, Liebmann JM, et al. Analysis of myocilin mutations in 1703 glaucoma patients from five different populations. *Hum Mol Genet*. 1999;8:899-905.
  8. Tamm ER. Myocilin and glaucoma: facts and ideas. *Prog Retin Eye Res*. 2002;21:395-428.
  9. Wang X, Johnson DH. mRNA in situ hybridization of TIGR/MYOC in human trabecular meshwork. *Invest Ophthalmol Vis Sci*. 2000;41:1724-1729.
  10. Takahashi H, Noda S, Mashima Y, et al. The myocilin (MYOC) gene expression in the human trabecular meshwork. *Curr Eye Res*. 2000;20:81-84.
  11. Swiderski RE, Ross JL, Fingert JH, et al. Localization of MYOC transcripts in human eye and optic nerve by in situ hybridization. *Invest Ophthalmol Vis Sci*. 2000;41:3420-3428.
  12. Huang W, Jaroszewski J, Ortego J, Escibano J, Coca-Prados M. Expression of the TIGR gene in the iris, ciliary body, and trabecular meshwork of the human eye. *Ophthalmic Genet*. 2000;21:155-169.
  13. Cheng EL, Ueda J, Wentz-Hunter K, Yue BYJT. Age independent expression of myocilin in the human trabecular meshwork. *Int J Mol Med*. 2002;10:33-40.
  14. Ueda J, Wentz-Hunter KK, Yue BYJT. Ultrastructural localization of myocilin in human trabecular meshwork cells and tissues. *J Histochem Cytochem*. 2000;48:1321-1329.
  15. Ueda J, Wentz-Hunter KK, Yue, BYJT. Distribution of myocilin and extracellular matrix components in the juxtacanalicular tissue of human eyes. *Invest Ophthalmol Vis Sci*. 2002;43:1068-1076.
  16. Lütjen-Drecoll E, Futa R, Rohen JW. Ultrahistochemical studies on tangential sections of the trabecular meshwork in normal and glaucomatous eyes. *Invest Ophthalmol Vis Sci*. 1981;21:563-573.
  17. Rohen JW, Futa R, Lütjen-Drecoll E. The fine structure of the cribriform meshwork in normal and glaucomatous eyes as seen in tangential sections. *Invest Ophthalmol Vis Sci*. 1981;21:574-585.
  18. Lütjen-Drecoll E, Shimizu T, Rohrbach M, Rohen JW. Quantitative analysis of "plaque material" in the inner and outer wall of Schlemm's canal in normal and glaucomatous eyes. *Exp Eye Res*. 1986;42:443-455.
  19. Rohen JW. Why is intraocular pressure elevated in chronic simple glaucoma? Anatomical consideration. *Ophthalmology*. 1983;90:758-765.
  20. Alvarado JA, Yun AJ, Murphy CG. Juxtacanalicular tissue in primary open-angle glaucoma and in nonglaucomatous normals. *Arch Ophthalmol*. 1986;104:1517-1528.
  21. Rohen JW, Lütjen-Drecoll E, Flügel C, Meyer M, Grierson I. Ultrastructure of the trabecular meshwork in untreated cases of primary open-angle glaucoma (POAG). *Exp Eye Res*. 1993;56:683-692.
  22. Lütjen-Drecoll E. Functional morphology of the trabecular meshwork in the primate eyes. *Prog Retin Eye Res*. 1998;18:91-119.
  23. Tripathi RC. The functional morphology of the outflow systems of ocular and cerebrospinal fluids. *Exp Eye Res*. 1997;25(suppl):65-116.
  24. Bill A. The drainage of aqueous humor. *Invest Ophthalmol Vis Sci*. 1975;14:1-3.
  25. Lütjen-Drecoll E, Rohen JW. Morphology of aqueous outflow pathways in normal and glaucomatous eyes. In: Ritch R, Shields MB, Krupin T, eds. *The Glaucomas*. St. Louis: Mosby; 1996:89-123.
  26. Lütjen-Drecoll E, Rittig M, Rauterberg J, Jander R, Mollenhauer J. Immunomicroscopical study of type VI collagen in the trabecular meshwork of normal and glaucomatous eyes. *Exp Eye Res*. 1989;48:139-147.
  27. Kuznetsov SA, Mankani MH, Gronthos S, Satomura K, Bianco P, Gehron Robey P. Circulating skeletal stem cells. *J Cell Biol*. 2001;153:1133-1139.
  28. Hann CR, Springett MJ, Johnson DH. Antigen retrieval of basement membrane proteins from archival eye tissues. *J Histochem Cytochem*. 2001;49:475-482.
  29. Gong H, Trinkaus-Randall V, Freddo TF. Ultrastructural immunocytochemical localization of elastin in normal human trabecular meshwork. *Curr Eye Res*. 1989;8:1071-1082.
  30. Cleary EG, Gibson MA. Elastin-associated microfibrils and microfibrillar proteins. *Int Rev Connect Tis Res*. 1993;10:197-209.
  31. Gibson MA, Sandberg LB, Grosse LE, Cleary EG. Complementary DNA cloning establishes microfibril-associated glycoprotein (MAGP) to be a discrete component of the elastin-associated microfibrils. *J Biol Chem*. 1991;266:7596-7601.
  32. Schwartz E, Goldfischer S, Coltoff-Schiller B, Blumenfeld O. Extracellular matrix microfibrils are composed of core proteins coated with fibronectin. *J Histochem Cytochem*. 1985;33:268-274.
  33. Kiely CM, Whittaker SP, Shuttleworth CA. Fibrillin: evidence that chondroitin sulphate proteoglycan are components of microfibrils and associate with newly synthesized monomers. *FEBS Lett*. 1996;386:169-173.
  34. Trask BC, Trask TM, Broekelmann T, Mecham RP. The microfibrillar proteins MAGP-1 and fibrillin-1 form a ternary complex with the chondroitin sulphate proteoglycan decorin. *Mol Biol Cell*. 2000;11:1499-1507.
  35. Hann CR, Springett MJ, Wang X, Johnson DH. Ultrastructural localization of collagen IV, fibronectin, and laminin in the trabecular meshwork of normal and glaucomatous eyes. *Ophthalmic Res*. 2001;33:314-324.
  36. Marshall GE, Konstas AG, Lee WR. Immunogold localization of type IV collagen and laminin in the aging human outflow system. *Exp Eye Res*. 1990;51:691-699.
  37. Marshall GE, Konstas AGP, Lee WR. Immunogold ultrastructural localization of collagens in the aged human outflow system. *Ophthalmology*. 1991;98:692-700.
  38. Murphy CG, Yun AJ, Newsome DA, Alvarado JA. Localization of extracellular proteins of the human trabecular meshwork by indirect immunofluorescence. *Am J Ophthalmol*. 1987;104:33-43.
  39. Fautsch MP, Johnson DH. Characterization of myocilin-myocilin interactions. *Invest Ophthalmol Vis Sci*. 2001;42:2324-2331.
  40. Wentz-Hunter K, Ueda J, Yue BYJT. Protein interactions with myocilin. *Invest Ophthalmol Vis Sci*. 2002;43:176-182.
  41. Tawara A, Okada Y, Kubota T, et al. Immunohistochemical localization of MYOC/TIGR protein in the trabecular tissue of normal and glaucomatous eyes. *Curr Eye Res*. 2000;21:934-943.
  42. Filla MS, Liu X, Nguyen TD, et al. In vitro localization of TIGR/MYOC in trabecular meshwork extracellular matrix and binding to fibronectin. *Invest Ophthalmol Vis Sci*. 2002;43:151-161.
  43. Hynes RO. *Fibronectins*. New York: Springer-Verlag; 1990.
  44. Rohen JW, Linner E, Witmer R. Electron microscopic studies on the trabecular meshwork in two cases of corticosteroid-induced glaucoma. *Exp Eye Res*. 1973;17:19-31.
  45. Johnson D, Gottanka J, Flügel C, Hoffmann F, Futa R, Lütjen-Drecoll E. Ultrastructural changes in the trabecular meshwork of human eyes treated with corticosteroids. *Arch Ophthalmol*. 1997;115:375-383.